



# Experimental and numerical investigation of the thermal performance of a protected vacuum-insulation system applied to a concrete wall

T. Nussbaumer \*, K. Ghazi Wakili, Ch. Tanner <sup>1</sup>

*Laboratory for Applied Physics in Building, EMPA, Swiss Federal Laboratories for Materials Testing and Research, Ueberlandstrasse 129, CH-8600 Duebendorf, Switzerland*

Received 27 May 2005; received in revised form 6 August 2005; accepted 13 August 2005  
Available online 14 October 2005

---

## Abstract

A concrete wall externally insulated with six expanded polystyrene boards, each containing three vacuum insulation panels, was investigated both experimentally and numerically. The main goal of this study was to determine the thermal performance of vacuum-insulation panels applied to walls in building constructions. Comparisons were made with conventional insulation and also with systems including damaged, i.e., vented vacuum panels. Since the vacuum insulation panels are encased in a metallized laminates as barriers against permeation of moisture and gas, special attention was given to the edge effects. Stepwise adjustment of the measured and calculated results reported here provide a general assessment of the efficacy of this insulation system applied on different wall materials. A functional representation of the measured data, for steady-state conditions, is introduced. Moreover, infrared thermography was used to confirm the three dimensionally calculated temperature distributions on the surface. The present investigation was part of the research programme “High Performance Thermal Insulation in Buildings and Building Systems” of the international energy agency (IEA).

© 2005 Elsevier Ltd. All rights reserved.

*Keywords:* Highly insulated walls; Vacuum-insulation panels; Edge effect; Linear thermal transmittance; *U*-value; Guarded hot-box

---

\* Corresponding author. Fax: +41 44 823 40 09.

*E-mail address:* [thomas.nussbaumer@empa.ch](mailto:thomas.nussbaumer@empa.ch) (T. Nussbaumer).

<sup>1</sup> Present address: QC-Expert, Kriesbachstrasse 42, CH-8600 Duebendorf, Switzerland.

## 1. Introduction

Since the end of the 1990s, a new type of highly insulating material [1,2] the so-called vacuum insulation panels (VIP) has been developed and introduced to construction technology. The most alluring feature of VIPs is their 5–10 times higher thermal resistivity for heat flow perpendicular to the main faces compared to conventional thermal insulation. This property opens the field for slim, energy efficient building envelope design which allows to enlarge the useable inner room sizes for a given exterior construction volume without reducing the thermal comfort.

The VIP consists basically of a micro-porous core structure which is vacuum-packed and encased in a multi-component barrier envelope (Fig. 1). This has to be gas and moisture tight in order to maintain the low thermal conductivity of the core.

While, during a first development period, an open-celled polystyrene foam has been used as core material, fumed silica powder ( $\text{SiO}_2$  agglomerate) has become nowadays the main core component in VIP applications in buildings. One of the reasons for the choice of this material is the fact that, compressed to about  $200 \text{ kg/m}^3$ , the pore size between the  $\text{SiO}_2$  grains is well below the mean free path of atmospheric gas molecules at internal pressures of 1–10 mbar. Thus heat transfer by convection [3,4] is minimized and limited to conduction ( $2\text{--}3 \text{ mW m}^{-1} \text{ K}^{-1}$ ) in the solid matrix, and thermal radiation. The latter is further reduced to about  $1 \text{ mW m}^{-1} \text{ K}^{-1}$  by the admixture of an opacifier to the basic fumed silica powder. The barrier envelopes have also been improved continuously by downsizing the thickness of the aluminum film from around  $10 \mu\text{m}$  to about  $90 \text{ nm}$ . This in turn reduces the lateral heat losses. Simultaneously to these improvements, investigations on the aging mechanisms and the service life of these widely-used barriers have been discussed [3]. Even though the improvement of the VIP barrier film is still ongoing [5,6], its vulnerability to mechanical stress usually encountered on building sites and to the welding seams as a potential source of leakages remains. This requires special protection measures not only during the construction period but also over the entire building lifespan.

Ideally, VIP units should be covered by a protective layer, as was the case for the panels examined in this study, where the VIPs were completely embedded in expanded polystyrene (EPS) preventing handling damage (scratches, cracks in the aluminum layer, etc.) to the foil as well as additionally screening the VIP from moisture. The present investigation set out to determine the impact of VIPs on the overall thermal behaviour of a wall

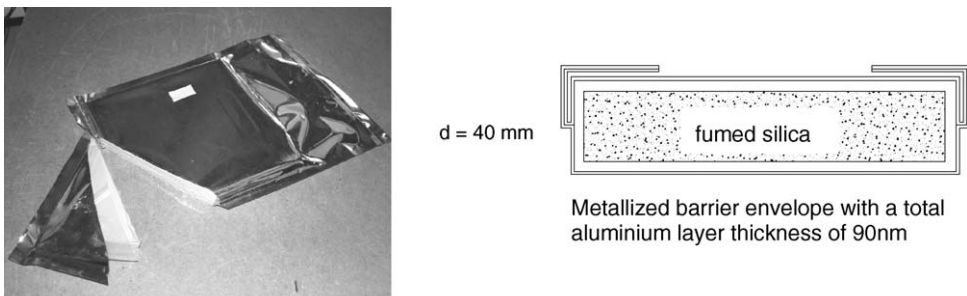


Fig. 1. Cross-section through a corner of the used VIP type with associated schematic sketch.

system for both intact and damaged cases. Hence hot-box measurements and steady-state 3D calculations have been carried out in parallel and their results are compared. A functional representation of the influence of damaged VIPs is given as well.

## 2. Experimental set-up

The thermal transmittance measurements were carried out using a guarded hot-box apparatus complying with the international standard ISO 8990 [7]. The overall opening of the apparatus was 2.680 m in width  $\times$  3.080 m in height and the centrally-positioned metering area was 2.003 m (width)  $\times$  2.504 m (height). The metering zone was surrounded by a guard zone held at a stable temperature. The wall system was incorporated in a surround panel made of an insulation material of known thermal properties and was fully encompassed by the metering area on the warm side (Fig. 2). Although the wall dimensions (1.500 m width  $\times$  2.000 m height) were in agreement with the opening of the surround panel, they were not identical to those of the metering area in order to account for edge effects. Hence allowance had to be made for the heat-flow component through the surrounding panel when analyzing the results.

As prescribed by the international standard ISO 12567-1 [8], a set of six calibrations was performed prior to the main measurement to determine the thermal resistance  $R_{\text{sur}}$  of the surrounding panel (Fig. 3) and the convective fractions on either side [8]. Additionally to

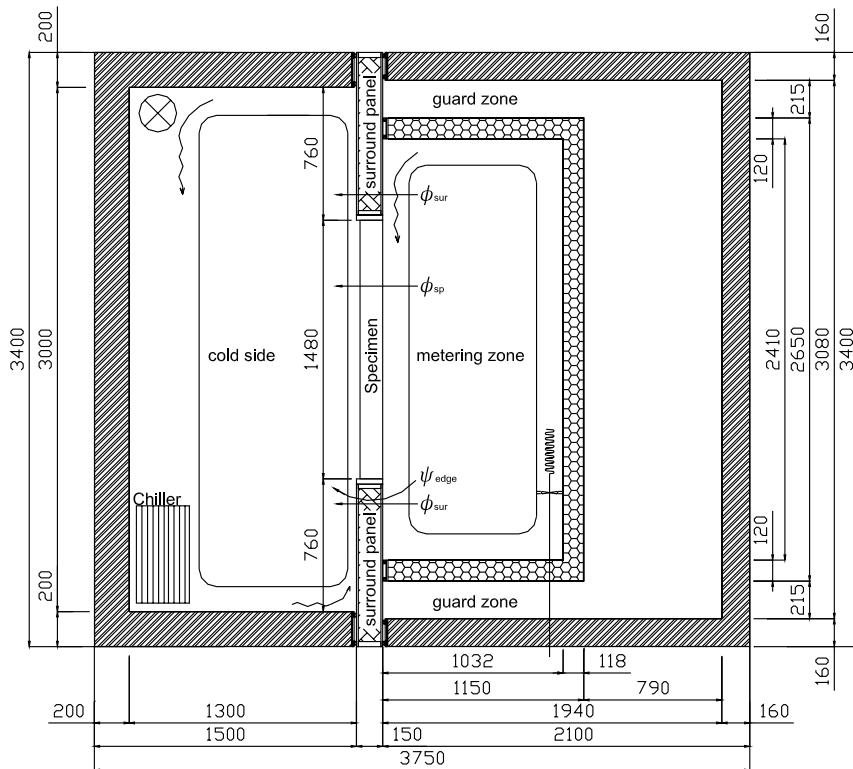


Fig. 2. Schematic vertical cross-section of guarded hot-box apparatus (dimensions in mm).

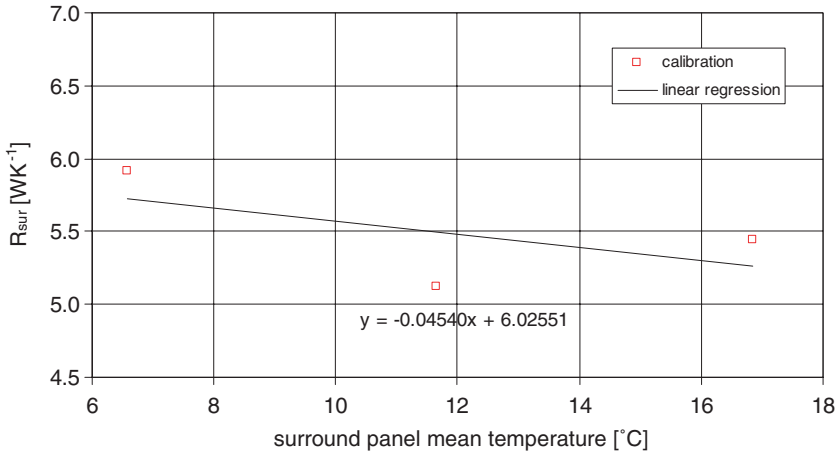


Fig. 3. Thermal resistance  $R_{sur}$  of the surrounding panel as a result of preceding calibrations.

these prescriptions, surface temperatures were measured and the total surface resistance was determined based on these values and the heat flux through the specimen. As the specimen and the surrounding panel had about the same thickness there was no reveal depth. This means that the radiation temperature on both cold and warm side was equal to the respective baffle temperature.

### 3. Specimen

A dry concrete wall (4 years old) of 18 cm thickness was used as the massive part of seven different sample configurations. Two layers of steel reinforcement were embedded in it at depths of 8 and 3 cm below the surfaces of the cold and warm side respectively. The density of the wall (including the reinforcement) was 2390 kg/m<sup>3</sup>. In order to have a basic test as a reference for intercomparisons, the thermal transmittance of the non-insulated

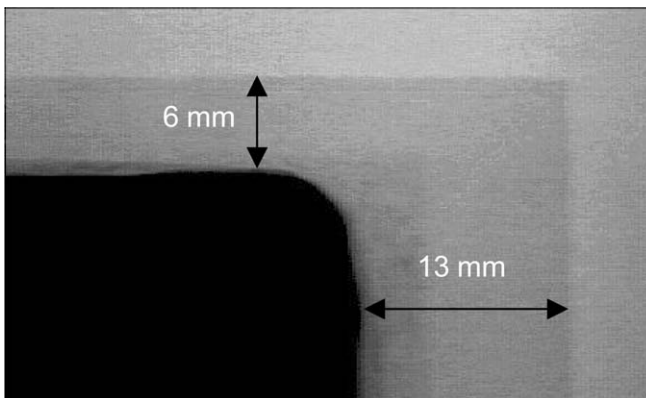


Fig. 4. X-ray radioscope of an edge of the insulating board containing VIPs. The dark part is caused by the aluminum layer in the barrier envelope of the VIP.

concrete wall was measured first. For the following tests, six insulation boards were applied to the concrete wall. These boards had the following outer dimensions:  $0.6\text{ m} \times 1.0\text{ m} \times 0.06\text{ m}$  (four pieces) and  $0.3\text{ m} \times 1.0\text{ m} \times 0.06\text{ m}$  (two pieces).

Each of these contained three 40 mm thick VIPs laying side by side and surrounded all over with a layer of EPS ( $\rho = 18.6\text{ kg/m}^3$ ) of about 1 cm thickness. Since the insulation boards were delivered as a whole, no information about the exact position of the VIPs within the boards was available. Instead of assuming an absolutely central position of the VIPs, the method of X-ray radioscopy was applied to all the boards. An example of this preliminary investigation is shown in Fig. 4. The resulting positions of the VIPs are shown in Fig. 5. The sizes of the single VIPs according to the manufacturer were:  $590\text{ mm} \times 330\text{ mm} \times 40\text{ mm}$  (12 pieces) and  $290\text{ mm} \times 330\text{ mm} \times 40\text{ mm}$  (six pieces).

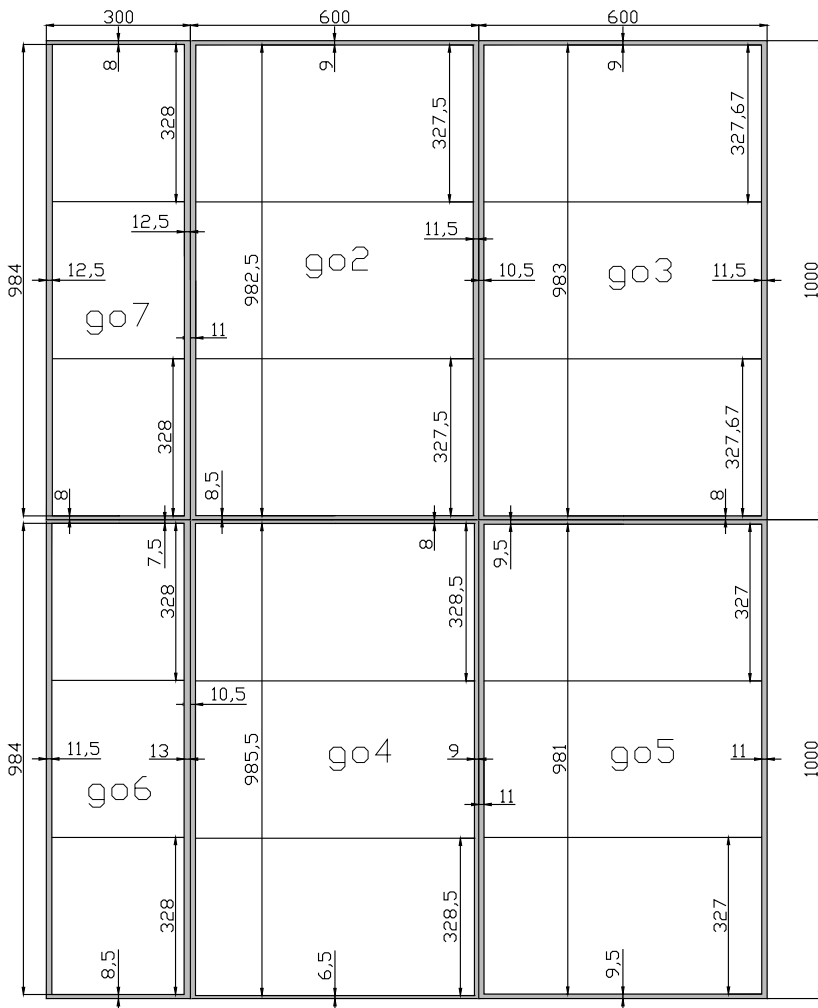


Fig. 5. Position of the VIPs (dimensions in mm) within the insulation boards (go2–go7 is the nomenclature of the boards, each containing three VIPs).

By reason of the technique used to form the VIPs it could be assumed that the VIPs were in the middle of the thickness of the insulation board, so that this position was not checked.

The VIPs were of the same type as pictured in Fig. 1 (metallized barrier envelope with a total aluminum layer thickness of 90 nm).

To increase the thermal performance of the concrete wall, six insulation boards were glued to the cold side of the concrete wall, similar to a conventional external thermal insulation composite system (ETICS). For this purpose, plaster of about 10 mm thickness was applied in stripes only (Fig. 6). On top of the insulation boards a layer of 6 mm thickness of plaster was evenly applied. A mesh was also embedded in this layer of plaster. Four days later a final layer of external plaster was put on the wall system. A detailed vertical cross section including all measures is outlined in Fig. 7. The measurements and calculations were carried out for seven different configurations and temperature differences  $\Delta T$  over the sample:

- (1) non-insulated concrete wall with  $\Delta T$  of about 20 K;
- (2) concrete wall with intact VIPs and  $\Delta T$  of about 20 K;
- (3) concrete wall with intact VIPs and  $\Delta T$  of about 40 K;
- (4) concrete wall with the middle VIP of go3 (Fig. 5) damaged (vented) and  $\Delta T$  of about 40 K;
- (5) concrete wall with three VIPs (go3 in Fig. 5) damaged and  $\Delta T$  of about 40 K;
- (6) concrete wall with six VIPs (go3 and go4 in Fig. 5) damaged and  $\Delta T$  of about 40 K;
- (7) concrete wall with nine VIPs (go3, go4 and go2 in Fig. 5) damaged and  $\Delta T$  of about 40 K.



Fig. 6. Plaster stripes on the insulation board to glue it onto the concrete wall.

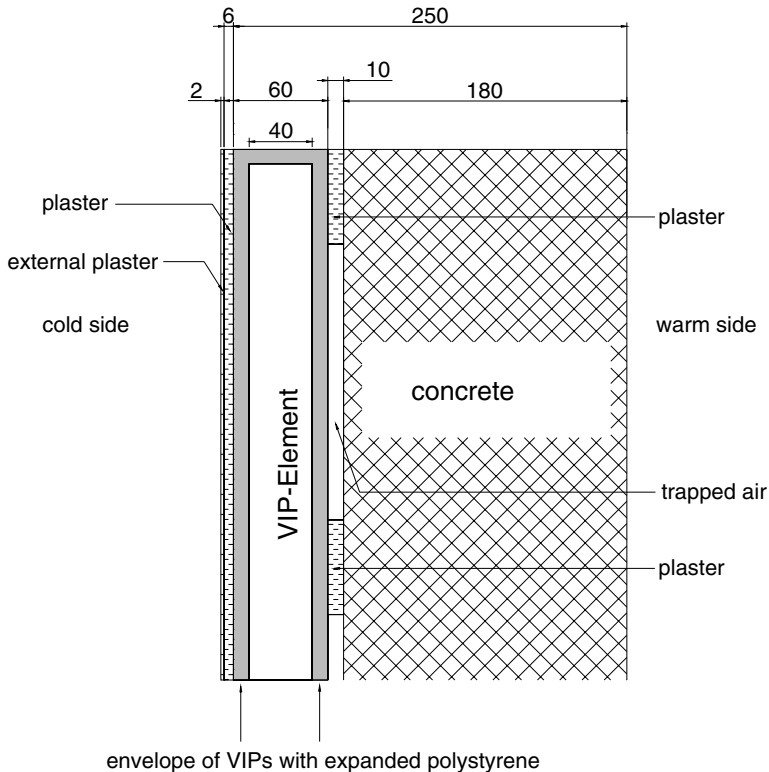


Fig. 7. Cross-section detail of the investigated wall (dimensions in mm).

For all these configurations the concrete wall was not dismantled from the surrounding panel, thus ruling out any potential errors due to mounting and handling operations. To damage the VIPs, a 2.5-mm diameter 35 mm deep hole was drilled into each panel.

#### 4. Visualisation by infrared thermography

Infrared thermography was used to visualize the surface temperature distribution of the specimen. This supplied information on the weak points and the influence of damaged VIPs compared to intact ones, as both were likely to leave an imprint on the temperature distribution. A further advantage of IR thermography was the possibility of checking air tightness at the junctions between the specimen and the surrounding panel. As a first check, IR pictures of the reference measurement (case 1) were mapped to find out whether the concrete reinforcement buried to a depth of 8 cm beneath the cold side of the wall affected the surface temperature distribution. Hence, the cold side of the hot box was moved aside after each measurement while the specimen remained connected to the warm side under unchanged thermal conditions. Given the fact that the laboratory temperature was around 22 °C, it is easily understandable that the predominant temperature difference of approximately 40 K could only be maintained shortly after opening the hot box. Therefore the IR pictures had to be taken very quickly (within one minute). It would have been

possible to take IR pictures from the warm side of the hot box, where conditions would remain stable after opening the hot box, but the thermal conductivity of concrete ( $1.87 \text{ W m}^{-1} \text{ K}^{-1}$ ) would blur the apparent influence of weak spots and damaged VIPs too much.

## 5. Numerical analysis

Numerical analysis was carried out for all seven configurations including the metering zone of the hot box using the TRISCO program [9], which calculates the three-dimensional steady-state heat-transfer in objects described in a rectangular grid using the energy-balance technique. The most challenging task of this analysis was to develop a simplified yet adequate model, as the thinnest layers contained in the specimen had a thickness of 30 nm with a very high thermal-conductivity of  $230 \text{ W m}^{-1} \text{ K}^{-1}$  embedded in a material with a fairly low conductivity of  $0.0053 \text{ W m}^{-1} \text{ K}^{-1}$  (Table 1). These abrupt changes in size and thermal conductivity were accommodated by various simplifications such as combining three (30 nm) aluminum layers into a single 90 nm layer and a very fine mesh. The same approach was adopted for the substrate layers (different polymers) of the

Table 1

Thermal conductivities of used materials measured by means of a hot-plate apparatus or determined by hot-box measurements

Material	Thermal conductivity ( $\text{W m}^{-1} \text{ K}^{-1}$ )	Material	Thermal conductivity ( $\text{W m}^{-1} \text{ K}^{-1}$ )
Plywood of birch	0.16	Non-metallic part of VIP foil	0.23 <sup>a</sup>
Expanded polystyrene ( $\rho = 18.6 \text{ kg/m}^3$ )	0.0335	Aluminum coated	230 <sup>a</sup>
Reinforced concrete	1.87 <sup>b</sup>	Polyethylene (low-density)	0.32 <sup>a</sup>
Plaster	0.29 <sup>a</sup>	VIP core-material intact	0.0053 <sup>b</sup>
External plaster	0.7 <sup>a</sup>	VIP core-material damaged	0.020 <sup>b</sup>

<sup>a</sup> Values given by manufacturer or the literature [12].

<sup>b</sup> Values resulting from comparison between measurement and calculation.

Table 2

Measured boundary conditions used as input for the numerical calculations

Case	Specimen description	Cold side		Warm side	
		$\theta_{\text{nc}}$ (°C)	$h_e$ ( $\text{W m}^{-2} \text{ K}^{-1}$ )	$\theta_{\text{ni}}$ (°C)	$h_i$ ( $\text{W m}^{-2} \text{ K}^{-1}$ )
1	Non-insulated concrete wall with $\Delta T$ of about 20 K	2.10	20.82	21.23	8.60
2	Concrete wall with intact VIPs and $\Delta T$ of about 20 K	2.05	21.83	21.97	6.76
3	Concrete wall with intact VIPs and $\Delta T$ of about 40 K	-17.82	21.20	21.85	7.11
4	Concrete wall with the middle VIP of go3 (Fig. 5) damaged and $\Delta T$ of about 40 K	-17.80	15.42	21.83	7.24
5	Concrete wall with all three VIPs of go3 (Fig. 5) damaged and $\Delta T$ of about 40 K	-17.82	16.87	21.80	7.33
6	Concrete wall with all six VIPs of go3 and go4 (Fig. 5) damaged and $\Delta T$ of about 40 K	-17.84	15.73	21.78	7.45
7	Concrete wall with all nine VIPs of go3, go4 and go2 (Fig. 5) damaged and $\Delta T$ of about 40 K	-17.83	14.35	21.75	7.50

barrier envelope. The area of the joint around each of the 18 VIPs was handled using a special simplified model [10]. Even so, the modelling ended with a total of about 2.3 million nodes which made it necessary to validate the results by other means than the proposed accuracy check stated in the standard EN ISO 10211-1 [11]. The thermal conductivities of the materials used in the model, as shown in Table 1, were either based on tabulated values [12] or found by stepwise adjustment and comparison with measurements [10]. The boundary conditions (environmental temperatures and surface heat-transfer coefficients) used for the numerical analysis corresponded with the values of the measurement (Table 2). As the specimen with the insulation boards filled the whole depth of the surrounding panel, there was no need to use partly reduced surface coefficients in the simulations.

## 6. Stepwise evaluation of measurement and numerical analysis

As the two investigation methods (measurement and calculation) are complementary, a stepwise evaluation method was used to determine the edge heat-loss for each measured configuration, the effective thermal conductivity of the reinforced concrete and of the intact as well as the damaged (vented) VIP core. For each measurement, three numerical calculations were carried out:

The first including the wall and the surrounding panel, was adjusted to the measurement by varying the effective thermal-conductivity of the reinforced concrete ( $i = 1$ : configuration 1), the thermal conductivity of the intact VIP ( $i = 2$ : configuration 2) and of the damaged VIP core ( $i = 4$ : configuration 4)

$$\Phi_{\text{in,c}} = \Phi_{\text{sur,c}} + \Phi_{\text{sp,c}}(\lambda_i) + \Psi_{\text{edge}}(\lambda_i) \cdot L_{\text{edge}} \cdot \Delta T_n, \quad (1)$$

where  $\Phi_{\text{in,c}}$  is the calculated total heat-flow rate [W],  $\Phi_{\text{sur,c}}$  the calculated heat-flow rate through the surrounding panel only [W],  $\Phi_{\text{sp,c}}$  the calculated heat-flow rate through the specimen only [W],  $\Psi_{\text{edge}}$  the calculated linear thermal-transmittance [ $\text{W m}^{-1} \text{K}^{-1}$ ],  $\Delta T_n$  = environmental temperature difference [K],  $L_{\text{edge}}$  is the joint length of surrounding panel and specimen [m](=perimeter of the specimen).

The second calculation accounted for the specimen only and ignored the surrounding panel by setting adiabatic boundary-conditions instead. This provided the value of the heat-flow rate through the specimen only ( $\Phi_{\text{sp,c}}$ ). Finally the surrounding panel alone was the object of the third calculation yielding the value of the heat-flow rate through it ( $\Phi_{\text{sur,c}}$ ). The linear thermal-transmittance ( $\Psi_{\text{edge}}$ ) of the wall could thus be determined by solving Eq. (1) for  $\Psi_{\text{edge}}$ .

The so calculated linear thermal-transmittance was used to determine the measured  $U$ -value of the specimen ( $U_{\text{W,m}}$ ) according to Eqs. (2) and (3):

$$U_{\text{W,m}} = \frac{(\Phi_{\text{in,m}} - \Phi_{\text{sur,m}} - \Phi_{\text{edge}})}{\Delta T_n \cdot A}, \quad (2)$$

where  $U_{\text{W,m}}$  is the measured  $U$ -value of the wall including the insulation boards [ $\text{W m}^{-2} \text{K}^{-1}$ ],  $\Phi_{\text{in,m}}$  the measured total heat flow rate input [W],  $\Phi_{\text{sur,m}}$  the measured heat-flow rate through the surround panel only [W],  $\Phi_{\text{edge}}$  the heat flow rate through the edge zone between the specimen and the surround panel [W] and  $A$  is the area of the specimen [ $\text{m}^2$ ].

$$\Phi_{\text{edge}} = L_{\text{edge}} \cdot \psi_{\text{edge}} \cdot \Delta T_c, \quad (3)$$

where  $\Delta T_c$  is the measured air temperature difference across the specimen [K] and  $\Psi_{\text{edge}}$  is the calculated linear thermal-transmittance [ $\text{W m}^{-2} \text{K}^{-1}$ ].

This measured  $U$ -value was compared to the calculated  $U$ -value resulting from Eq. (4):

$$U_{\text{W,c}} = \frac{\Phi_{\text{sp,c}}}{\Delta T_n \cdot A}. \quad (4)$$

## 7. Results and discussion

The application of the above procedure to configurations 1, 2 and 4 resulted in equivalent thermal-conductivities for the reinforced concrete of  $1.87 \text{ W m}^{-1} \text{K}^{-1}$ , the intact VIP core of  $0.0053 \text{ W m}^{-1} \text{K}^{-1}$  and the damaged VIP core of  $0.020 \text{ W m}^{-1} \text{K}^{-1}$  (see values with a superscripted b in Table 1) which were close to the reported value of another study on a VIP equipped specimen [13].

The value for the undamaged VIP core is somewhat higher than the average value of  $0.0043 \text{ W m}^{-1} \text{K}^{-1}$  reported in [10], but the determination of the thermal conductivity of some dismantled VIPs (without the surrounding EPS) performed in a guarded hot-plate device, after having finished the  $U$ -value measurements, resulted in a value of  $0.0049 \text{ W m}^{-1} \text{K}^{-1}$  with an internal pressure of the VIPs of 3–4.5 mbar. This higher thermal conductivity compared to the values given in [10] is most likely due to a VIP core which was less extensively dried. Such an influence of the water content of the VIP core to the thermal conductivity is published in [3,4].

Table 3  
Measurements and calculated results

Case	Specimen description	$\Phi_{\text{in,m}}$ (W)	$\Phi_{\text{in,c}}$ (W)	$U_{\text{W,m}}$ ( $\text{W m}^{-2} \text{K}^{-1}$ )	$U_{\text{W,c}}$ ( $\text{W m}^{-2} \text{K}^{-1}$ )	$U_{\text{W,st}}$ ( $\text{W m}^{-2} \text{K}^{-1}$ )
1	Non-insulated concrete wall with $\Delta T$ of about 20 K	228.91	228.78 <sup>a</sup>	$3.83 \pm 0.08$	3.84	3.74
2	Concrete wall with intact VIPs with $\Delta T$ of about 20 K	18.83	18.50 <sup>a</sup>	$0.16 \pm 0.01$	0.17	0.16
3	Concrete wall with intact VIPs and $\Delta T$ of about 40 K	36.86	36.65	$0.16 \pm 0.01$	0.17	0.17
4	Concrete wall with the middle VIP of go3 (Fig. 5) damaged and $\Delta T$ of about 40 K	38.97	38.01 <sup>a</sup>	$0.18 \pm 0.01$	0.18	0.19
5	Concrete wall with all three VIPs of go3 (Fig. 5) damaged and $\Delta T$ of about 40 K	42.05	41.01	$0.21 \pm 0.01$	0.21	0.21
6	Concrete wall with all six VIPs of go3 and go4 (Fig. 5) damaged and $\Delta T$ of about 40 K	46.41	45.55	$0.25 \pm 0.02$	0.25	0.25
7	Concrete wall with all nine VIPs of go3, go4 and go2 (Fig. 5) damaged and $\Delta T$ of about 40 K	50.84	49.89	$0.29 \pm 0.01$	0.29	0.29

<sup>a</sup> These values are adjusted.

Based on the above stated values for the thermal conductivity of the materials used, a comparison between calculated values and measurements was done for configurations 3, 5, 6 and 7 (Table 3) by means of the  $U$ -value which is the standard parameter for building elements in real applications.

It is immediately noticeable that the measured (column 3) and the calculated (column 4) total heat-flow rates lie extremely close. This shows clearly that the adjustments made for cases 1, 2 and 4 between measurements and calculations were appropriate to provide a good degree of concordance for the cases 3, 5, 6 and 7.

The influence of the damaged VIPs on the  $U$ -value of the insulated wall (columns 5 and 6 for the cases 3–7) were plotted with respect to two different aspects (modified  $x$ -axis), namely:

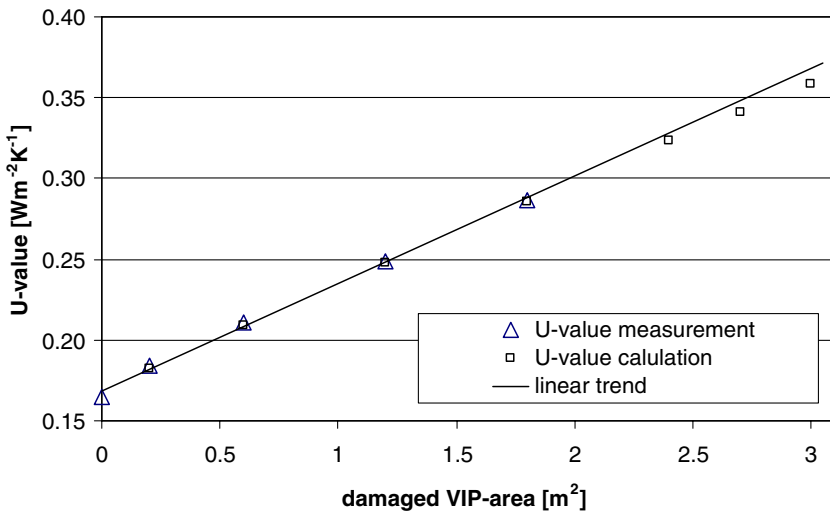


Fig. 8. Overall  $U$ -value of the insulated concrete wall as a function of damaged VIP-area.

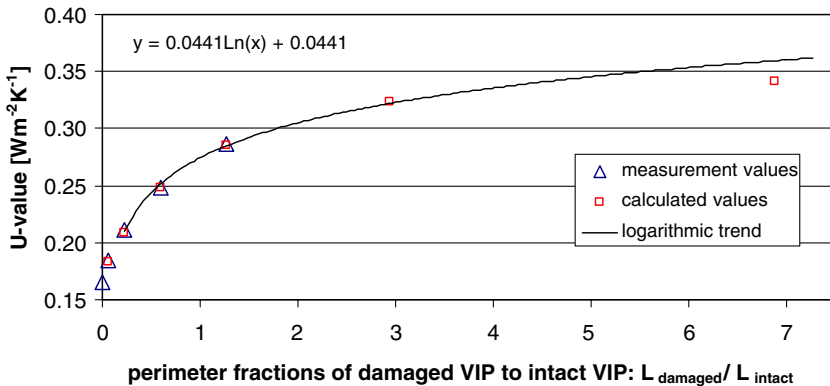


Fig. 9. Assessment of the influence of the ratio of the damaged VIP-perimeter to the intact VIP-perimeter.

- (a) Total damaged VIP-area (Fig. 8).  
 (b) The ratio of damaged to intact VIP-perimeter length:  $L_{\text{damaged}}/L_{\text{intact}}$  (Fig. 9).

To enable the extrapolation of these two plots beyond the measured cases, additional calculations were carried out for the maximum damaged VIP area. The almost linear behaviour of the  $U$ -value with increasing damaged VIP-area (Fig. 8) can be explained by the surrounding insulation material of the VIPs which dampens the edge effect of the adjacent VIPs within one board.

As  $U$ -values are usually reported as standardized heat-transfer coefficients, an appropriate conversion (Table 3, column 7) of the measured values (Table 3, column 5) was done according to Eq. (5):

$$U_{W,\text{st}} = \left[ U_{W,\text{m}}^{-1} + 0.17 - R_{s,\text{tot,m}} \right]^{-1}, \quad (5)$$

where  $U_{W,\text{m}}$  is the measured  $U$ -value of the wall including the insulation boards [ $\text{W m}^{-2} \text{K}^{-1}$ ], 0.17 the standardized total surface thermal resistance [ $\text{m}^2 \text{K W}^{-1}$ ] and  $R_{s,\text{tot,m}}$  is the measured total surface thermal resistance [ $\text{m}^2 \text{K W}^{-1}$ ].

Fig. 10 shows the improvement of a supporting construction by the application of the investigated VIP system as a function of the thermal resistance of the supporting construction according to Eq. (6):

$$U_W = \frac{1}{R_{\text{supconstr}} + R_{\text{Insulation}} + R_{\text{si}} + R_{\text{se}}}, \quad (6)$$

where all the following parameters are based on measurement:  $U_W$  is the  $U$ -value of the wall [ $\text{W m}^{-2} \text{K}^{-1}$ ],  $R_{\text{si}}$  the surface thermal resistance on the warm side [ $\text{m}^2 \text{K W}^{-1}$ ],  $R_{\text{se}}$  the measured surface thermal resistance on the cold side [ $\text{m}^2 \text{K W}^{-1}$ ],  $R_{\text{Insulation}}$  the mea-

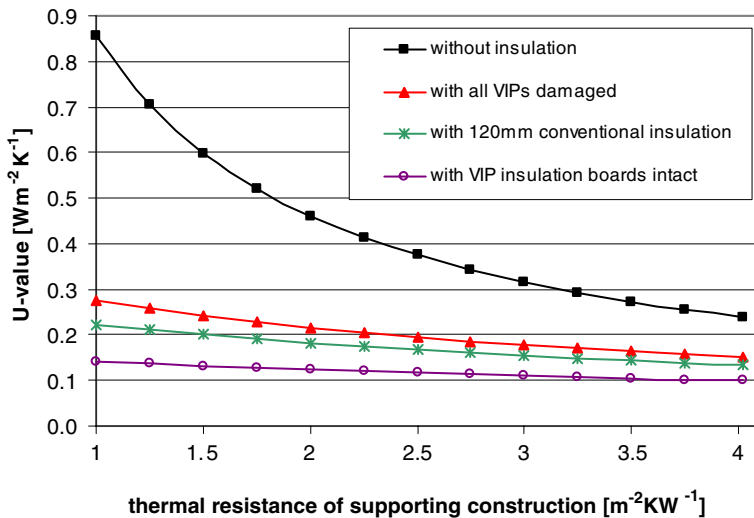


Fig. 10. Potential improvement by the applications of 60 mm-thick insulation boards containing VIPs which are half the thickness of a conventionally used insulation.

sured thermal resistance of the insulating layer [ $\text{m}^2 \text{K W}^{-1}$ ],  $R_{\text{sup constr}}$  is the measured thermal resistance of the supporting construction [ $\text{m}^2 \text{K W}^{-1}$ ].

This is valid for quasi-homogeneous supporting constructions such as concrete, porous concrete, etc., excluding constructions with severe thermal bridges, which can be confirmed by means of IR-thermography. Applying Eq. (6) to configuration 1, where  $R_{\text{Insulation}} = 0$ , results in the thermal resistance of the reinforced concrete  $R_{\text{concrete}} = 0.0972 \text{ m}^2 \text{K W}^{-1}$ . This value together with the application of Eq. (6) to configuration 2 leads to  $R_{\text{Insulation}} = 5.883 \text{ m}^2 \text{K W}^{-1}$ . Additionally the effect of a conventional insulation layer of 120 mm thickness and a thermal conductivity of  $0.036 \text{ W m}^{-1} \text{K}^{-1}$  was calculated and is represented in Fig. 10.

IR thermography showed no influence of the reinforcing rods on the temperature distribution of the cold side. As seen in Fig. 11 this method visualized the different thermal resistances of the intact VIP and the surrounding EPS as measured in case 3. A qualitative comparison between IR-detected and calculated surface temperature distribution for configuration 7 is given in Fig. 12. The damaged VIPs (boards: go2, go3 and go4) are clearly recognizable. It has to be mentioned that the boundary conditions are ideally homogeneous for the calculation, contrary to the unstable conditions shortly after opening the hot box for IR-thermography. The black dots on the IR image are due to some glue material left on the wall, having a different emissivity than the wall surface.

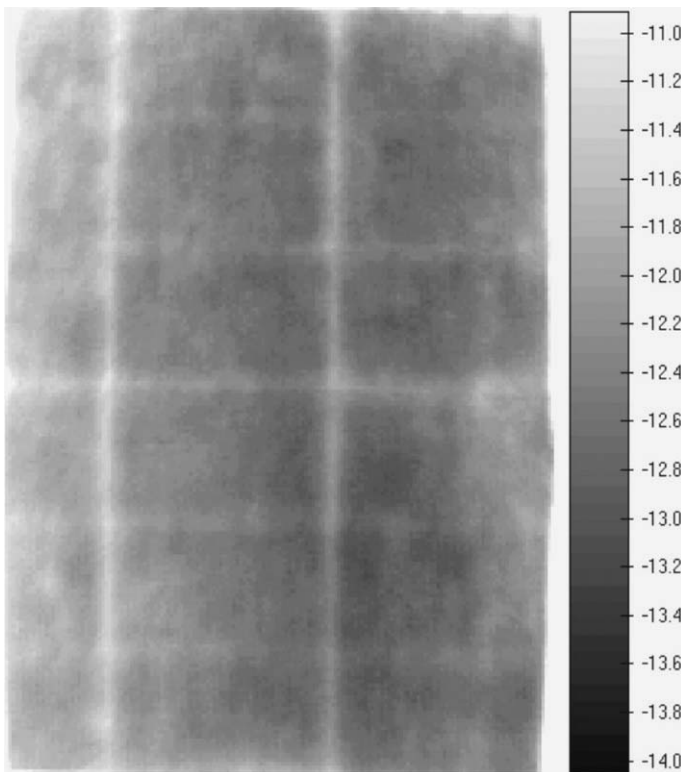


Fig. 11. Infrared (IR)-image (date 16.12.04; time 13:45:50) of the specimen's cold side (case 3). Scale to the right in degrees Celsius.

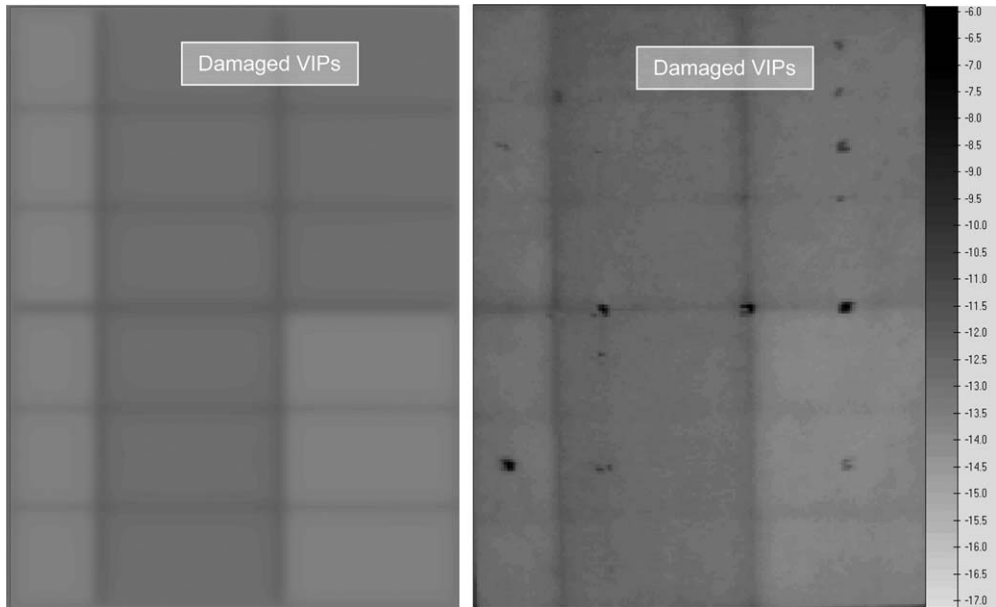


Fig. 12. Comparison of calculated (left) and infrared measured (right; date 24.02.2005; time 11:55:27) temperature distribution on the cold side of the wall for case 7. The darker areas (higher temperature) indicate damaged VIPs. The black dots are due to gluing material with a different emissivity. Scale to the right in degrees Celsius.

## 8. Conclusions and outlook

A safe and promising application of VIPs in buildings involves their use under a protective layer. One such an example investigated in this study is a system of VIPs embedded in EPS foam forming insulation boards mounted on an exterior wall.

The thermal analysis of this system was carried out both numerically and experimentally, and resulted in the following conclusions:

- A thermal improvement of over 95% was realized by adding a layer of 60 mm insulation boards containing 40 mm thick VIPs. Using conventional insulation, with a thermal conductivity of  $0.036 \text{ W m}^{-1} \text{ K}^{-1}$ , would require a total thickness of 212 mm (i.e. more than factor 3.5 thicker).
- Besides the protective role, the thickness enlarging EPS foam reduces the edge effect of the VIPs caused by the aluminum layers within their barrier envelope.
- Even if 60% of the VIPs should be damaged (i.e. no vacuum), the wall system still exhibits a  $U$ -value below  $0.3 \text{ W m}^{-2} \text{ K}^{-1}$ , so meeting the requirements for walls of new buildings in Switzerland. This would correspond to a thickness of 90 mm of conventional insulation.

The stepwise evaluation of measurements and calculations as practiced in this contribution, demonstrates clearly the benefit of this technique.

IR thermography can be used as an inspecting tool to recognize damaged VIPs when the difference between the external and internal temperature is above 20 K, i.e., winter conditions.

To develop another simple in situ method for checking the quality of implemented VIPs in already existing facades would be a step forward in promoting VIP technology.

### Acknowledgements

The present work was partly supported by the Swiss Federal Office of Energy. The authors are thankful to R. Bundi for preparing the numerical data input and to S. Brunner, H. Simmler and T. Frank for valuable discussions.

### References

- [1] Caps R, Heinemann U, Ehrmantraut M, Fricke J. Evacuated insulation panels filled with pyrogenic silica powders: properties and applications. *High Temp-High Press* 2001;33:151–6.
- [2] Simmler H. Measurement of physical properties of VIP. In: Zimmermann M, Bertschinger H, editors. High performance thermal insulation systems, vacuum insulated products (VIP). Proceedings of the international conference and workshop, Centre for energy and sustainability in buildings. Duebendorf (Switzerland): EMPA; 2001.
- [3] Simmler H, Brunner S. Vacuum insulation panels for building applications. *Energ Buildings*; 2005 [in press].
- [4] IEA/ECBCS Annex 39, Vacuum insulation panels, study on VIP-components and panels for service life prediction of VIP in building applications (Subtask A) [in press].
- [5] Carmi Y. Ultra high barrier films for long-term applications – the next generation. In: Proceedings to the VIA symposium in Atlanta. Vacuum Insulation Association; May 2002.
- [6] Brandt R. Innovationen mit Barrierefolien, Fachtagung Sperrschichtfolien in Würzburg, Germany; June/ July 2004.
- [7] ISO 8990. International Standard. Thermal insulation – determination of steady-state thermal transmission properties – calibrated and guarded hot box; 1994.
- [8] ISO 12567-1. International Standard. Thermal performance of windows and doors – determination of thermal transmittance by hot-box method – Part 1: complete windows and doors; 2000.
- [9] TRISCO Manual, Version 10.0 w, Physibel, Maldegem, Belgium; 2001.
- [10] Ghazi Wakili K, Bundi R, Binder B. Effective thermal conductivity of vacuum-insulation panels. *Building Res Inform* 2004;32:293–9.
- [11] EN ISO 10211-1 European and International Standard. Thermal bridges in building construction – heat flow and surface temperatures – Part 1: general calculation methods; 1995.
- [12] EN 12524 European standard. Building materials and products – hygrothermal properties – tabulated design values; 2000.
- [13] Nussbaumer T, Bundi R, Tanner Ch, Muehlebach H. Thermal analysis of a wooden-door system with integrated vacuum-insulation panels. *Energ Buildings*; 2005 [in press].